Numerical Investigation on Flow Control of Leading-Edge Reinforced Flexible Membrane Wing

Z. Liu1*, and WH. Xie2
State Key Laboratory of Mechanical Structural Strength and Vibration, Xi'an Jiaotong University, Xi'an, Shaanxi, China

http://www.imavs.org/

ABSTRACT

The leading-edge reinforced flexible membrane wing can reduce spanwise deformation and has the advantage of adaptive passive deformation of the membrane wing. A membrane wing with a certain thickness at the leading edge and an equal thickness at the trailing edge was designed. The membrane wing film thickness is 1mm and the ratio of the film area to the whole wing is 72.2%. The Fluid-Structure Interaction (FSI) analysis method was established, and the aerodynamic characteristics of the wing was studied. Results showed that the maximum deformation of the leading edge of the wing tip is 4.75%. The flow separation is delayed due to the deformation of the elastic film which improves the aerodynamic performance after stall. It is found that the leading-edge reinforced membrane wing deformed little in spanwise direction which reduces the deterioration of aerodynamic performance caused by spanwise deformation. The membrane wing near the trailing edge still has significant adaptive passive deformation resulting in the improvement of stall performance.

1 INTRODUCTION

In recent years, there are more and more researches on deformable wings, whose main goal is to improve the aerodynamic characteristics of traditional rigid wings, improve efficiency and expand the flight envelope. The traditional wing deformation concept mainly focuses on the deformation of flaps, ailerons and wing sweepback. Although the efficiency and flight envelope of the wing have been greatly improved, the added mass has increased, and the aerodynamic performance has declined due to discontinuities and gaps between components, which is particularly obvious in low-speed flight. The lightweight, low cost, and simple structure of membrane wings make them more promising in low-speed applications compared to traditional rigid wings [1]. In the mid-20th century, the Princeton sail appeared, also known as the double membrane sail, which was basically composed of a rigid leading edge spar and a trailing edge wire (or spar). The membrane wraps around the leading and trailing edges, forming the upper and lower wing surfaces. Originally conceived as an advanced sail, it was later transformed into an aircraft wing. Reference [2] conducted experimental tests on different sail configurations, and the results showed that the aerodynamic characteristics of membrane wings were superior to traditional rigid wings in terms of maximum lift and maximum lift drag ratio. A notable feature of membrane wings is their ability to naturally adjust their shape to adapt to constantly changing flow conditions, namely 'adaptive' passive deformation, resulting in excellent stall characteristics. In the study of membrane wings, many scholars have focused on the influence of the deformation of elastic membranes on aerodynamic performance. In their research, flat membrane wings with fixed peripheral frames are often used as research objects. For example, reference [3] studied the influence of membrane permeability characteristics on wing aerodynamic efficiency, and the results verified the possibility of dynamic pressure compensation through wing permeability. Fujita [4] proposed the "self consistent theory" and used it to predict the aerodynamic performance of flat membrane wings with fixed and free wingtips. This theory can effectively predict the deformation of elastic membranes and the lift hysteresis characteristics of flat membrane wings, and has good consistency with wind tunnel test data. Song [5] proposed a theoretical model for membrane bending caused by aerodynamic loads, indicating that the appropriate dimensionless parameter to describe the problem is the Weber number, which compares aerodynamic loads with membrane elasticity. It was found that the theory was very consistent with the experiment. Aerodynamic performance measurement shows that compared with rigid wings, flexible wings have higher lift slope, maximum lift coefficient and delayed stall at higher angles of attack. In addition, they exhibit strong hysteresis near zero angle of attack and stall angle. Mueller [6, 7] conducted research and analysis on curved flat membrane wings, demonstrating the importance of curvature and wing shape, indicating that the inverse Zimmerman shape is superior for low Re flow. Albertani [8] applied membrane wings to micro fixed wing unmanned aerial vehicles, developed and manufactured low aspect ratio wings, using an elastic latex film skin covered with a thin carbon fiber skeleton. The wings were tested in a low-speed wind tunnel facility that integrates a visual image correlation (VIC) system and a six component strain gauge balance. The static response characteristics of three different wing designs were measured, including full field displacement and plane strain measurements. The full field deforma-

*Email address(es): liuz@mail.xjtu.edu.cn

http://www.imavs.org/

tion results indicate how the flexibility of the passive wing better affects aerodynamic performance compared to rigid models with similar geometric shapes. Measure elastic deformation and aerodynamic coefficients through wind tunnel testing methods. Previous studies have shown that membrane wings have good aerodynamic performance at low Re, but when aerodynamic loads are high, membrane wings exhibit significant spanwise bending and torsion deformation, which is detrimental to aerodynamic performance. The main reason is limited by the small thickness of the membrane wing, and excessive size of the reinforcing ribs can easily cause discontinuity between the reinforcing ribs and the membrane wing. Therefore, the small thickness of the reinforcing ribs is prone to spanwise bending and torsion deformation. In response to this issue, this article proposes a hybrid membrane wing with leading edge reinforcement, which combines traditional airfoils and membrane wings to enhance spanwise stiffness while retaining the advantages of membrane wings' adaptive passive deformation. This article conducts a study on structural deformation based on the thickness and membrane ratio of this airfoil.

Due to the small stiffness of membrane wings, they undergo significant "adaptive" passive deformation under aerodynamic loads. The large deformation of the structure has a significant impact on the flow field, which in turn affects the aerodynamic performance of the wing. This is a typical fluid structure coupling problem. At present, there are two main methods for solving fluid solid coupling problems: direct coupled solution and partitioned solution. The direct coupling method solves the fluid solid control equations by coupling them into the same equation matrix, and simultaneously solving the control equations of the fluid and solid in the same solver. However, in practical applications, direct solutions face convergence difficulties and time-consuming issues in synchronous solutions. Therefore, they are currently mainly used in simple problems such as electromagnetic structural coupling and thermal structural coupling, such as piezoelectric material simulation. The separation method does not require coupling the fluid solid control equations, but solves the fluid control equations and the solid control equations separately in the same solver or different solvers in the set order. The calculation results of the fluid domain and the solid domain are exchanged and transmitted through the fluid solid interface (FS Interface). When the convergence at this moment meets the requirements, proceed with the calculation at the next moment and obtain the final result sequentially. Compared with the direct coupling method, the separation method has the disadvantages of time lag and incomplete conservation of energy on the coupling interface. However, the advantages of this method are also obvious. It can maximize the use of existing methods and programs of computational fluid dynamics and computational solid mechanics, and only need to make a few modifications to them, so as to maintain the modularization of the program.

The research results indicate that at high reduction frequencies, flexible airfoils have the characteristic of low drag, and their aerodynamic performance is significantly superior to that of rigid airfoils; The passive deformation of flexible airfoils can suppress the generation of surface vortices and optimize aerodynamic characteristics. Some researchers conducted wind tunnel experiments on flexible wings with high aspect ratio, studying their physical parameters such as lift resistance, displacement, vortex shedding frequency, suction surface, and wake vorticity field. Through experimental research, it was found that flexible wings with high aspect ratio exhibit similar characteristics to rigid wings under the same conditions in some aspects. In this study, due to the small stiffness of the elastic thin film and its significant deformation under aerodynamic loads, it is necessary to use the fluid solid coupling method for research. Considering the computational cost and convergence, a weak coupling solution method, namely the separation method, is adopted.

This article proposes a design concept for a leading edge reinforced bioinspired membrane wing, and establishes an aerodynamic model for the leading edge reinforced bioinspired membrane wing based on a structured grid flow field partitioning method. The finite element model for the leading edge reinforced bioinspired passive membrane wing is also developed, and flow control research on the leading edge reinforced bioinspired passive membrane wing is carried out through fluid structure coupling method.

2 COMPUTATIONAL METHODOLOGY

Establish a bidirectional FSI model for structural aerodynamics for further analysis. The structure aerodynamic bidirectional FSI model mainly includes structural model, aerodynamic flow field model, and structure aerodynamic data interaction platform. The structural model is a finite element model, which calculates the displacement deformation of the wing under aerodynamic loads and transmits the displacement deformation to the aerodynamic model through the structural aerodynamic data interaction platform; The aerodynamic model recalculates the flow field based on displacement deformation, obtains aerodynamic data (mainly aerodynamic pressure), and transmits it to the structure through the structure aerodynamic interaction platform; The structure recalculates displacement and deformation, iterating continuously until the residual meets the accuracy requirements. The flight speed in this article is between 15m/s and 20m/s, therefore it is considered that the surrounding fluid is incompressible. At the same time, its operating state is at low Reynolds number, and viscous force has a greater impact, so viscous effect is considered. A three-dimensional incompressible Navier Stokes control equation considering viscous effects for a hybrid membrane wing with reinforced leading edge is obtained comprehensively. The $k-\omega$ SST turbulence model is used. And a second-order discretization scheme was used as well. For membrane wing structure, the finite element

http://www.imavs.org/

method is used to discretize the structure in space, and Newmark method is used to solve it. Ansys software was used for the simulation.

3 COMPUTATIONAL MODEL OF LEADING-EDGE REINFORCED FLEXIBLE MEMBRANE WING

3.1 Introduction of Leading-Edge Reinforced Flexible Membrane Wing

When the flight Reynolds number is low, the membrane wing has better aerodynamic performance than the traditional airfoil. Traditional membrane wings are all curved thin plate structures with equal thickness. To enhance their load-bearing capacity, reinforcing ribs are added to the membrane wings. Generally, cylindrical reinforcing ribs are used at the leading edge, while narrow strip thin plate reinforcing ribs are used for the rest. When the aerodynamic load is small, this layout can meet the required bearing capacity, but when the aerodynamic load is large, the membrane wing will produce significant bending and torsional deformation, which reduces the aerodynamic performance of the membrane wing. Therefore, this article combines traditional airfoils with membrane wings, retaining the thickness of the leading edge of the traditional airfoil. The half of the airfoil adopts membrane wing design, resulting in a hybrid airfoil with strengthened leading edge, as shown in Figure 1.

Based on the above airfoil, a leading edge reinforced membrane wing was designed as shown in Figure 2. The wing has a span length of 0.6mm and a chord length of 0.12mm. The yellow part in the figure shows the surrounding support structure, composed of carbon fiber reinforced composite materials, which is the main structure of the leading edge reinforced hybrid membrane wing. The blue part in the figure is an elastic film composed of Dielectric elastomers (DE) material, mainly responsible for the adaptive passive deformation function of the membrane wing. The properties of DE materials and carbon fiber reinforced composite materials are shown in Table 1 and Table 2.

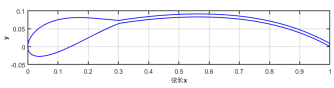

Figure 1: Leading-edge reinforced airfoil.

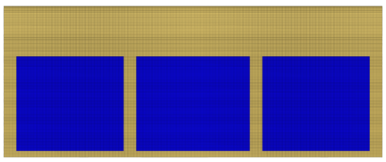

Figure 2: Leading-edge reinforced membrane wing.

$\rho(kg/m^3)$	$E_1(MPa)$	μ
960	0.748	0.47

Table 1: Material parameters of DE material.

$\rho(kg/m^3)$	$E_x(Pa)$	$E_y(Pa)$	$E_z(Pa)$	μ_{xy}
1300	4.2e10	4.2e10	1e10	0.35
μ_{yz}	μ_{xz}	$G_zy(Pa)$	$G_yz(Pa)$	$G_xz(Pa)$
0.3	0.3	2.1e10	7e9	7e9

Table 2: Material parameters of carbon fiber reinforced composites.

3.2 Aerodynamic Model and Structural Model

A three-dimensional aerodynamic model of the leading edge reinforced membrane wing was established, as shown in Figure 3. The front flow field of the wing is 10c, the rear flow field is 20c, and the upper and lower flow fields are 10c. The total number of grids is 7557116, all of which are hexahedral grids. The number of boundary layers is 10, and the thickness of the first layer is y+=1, i.e. 0.019mm. Establish a finite element model of the wing structure based on the geometry of the membrane wing, using hexahedral elements as the mesh type, which can truly reflect structural deformation and establish numerical interpolation relationships with the flow field, as shown in Figure 4. The middle part is an elastic film, and the surrounding part is the skeleton support structure of the membrane wing. The elastic film and the skeleton support structure are connected through the side, and the Bounded connection relationship is given to ensure consistent calculation efficiency and accuracy of the connection nodes. The strengthening part of the leading edge of the membrane wing is the connection part between the wing and the fuselage, so fixed constraints are given on the side of the wing root at the strengthening part of the leading edge.

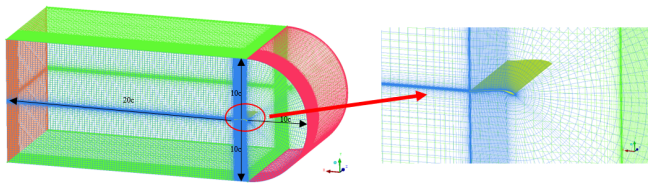

Figure 3: Aerodynamic mesh of the wing.

4 RESULTS AND DISCUSSION

In order to understand the aerodynamic characteristics of the membrane wing, the aerodynamic characteristics of rigid wing which did not consider the elasticity of wing and membrane wing were studied separately. The Reynolds number is 122262. Because the stall angle of the wing is about 12 °, the range of the angle of attack is from 10 ° to 20 °. Figures 5,

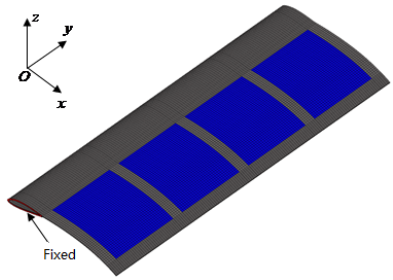

Figure 4: Structural mesh of the wing.

6 and 7shows the lift coefficient curve, drag coefficient curve and lift drag ratio curve of rigid wing and membrane wing at different angles of attacks.

Compared with the rigid wing aerodynamic results, the lift coefficient of the rigid wing before stall is greater than the lift coefficient of the leading edge strengthened hybrid membrane wing, which is mainly due to the passive deformation of the membrane wing under the effect of aerodynamic pressure. When it is greater than the stall angle of attack, the lift coefficient of the rigid wing is less than that of the leading edge strengthened hybrid film wing, and the stall angle of attack of the rigid wing is around 12 °, the stall angle of attack of the leading edge strengthened hybrid film wing is around 14 °, and the stall angle of attack is delayed by about 2 °. By comparing the lift coefficient decline after stall, it can be seen that the lift coefficient of the leading edge strengthened hybrid film wing decreases slightly, while the lift coefficient of the rigid wing decreases greatly. By comparing the drag coefficient, it can be seen that when the angle of attack is small, the drag coefficient of the leading edge reinforced mixed film wing is smaller than that of the rigid wing. By comparing the lift to drag ratio, it can be seen that the lift to drag ratio of the leading edge reinforced mixed film wing is greater than that of the rigid wing throughout the entire process, resulting in higher aerodynamic efficiency. Verified that the hybrid membrane wing with reinforced leading edge still retains the advantages of adaptive passive deformation of the membrane wing.

Figure 8 shows the pressure contour at the middle section of a rigid wing and a leading edge reinforced mixed membrane wing at different angles of attack, where a is the rigid wing and b is the leading edge reinforced mixed membrane wing. According to the pressure cloud map, the pressure difference between the upper and lower surfaces of the wing is mainly concentrated at the leading edge, so the lift is mainly distributed at the leading edge. However, due to the traditional airfoil used for strengthening the leading edge, it has strong resistance to spanwise bending deformation and has small displacement deformation at the leading edge of the wing tip. Comparing the pressure cloud maps of a rigid wing and a hybrid membrane wing with a strengthened leading edge after stall (angle of attack greater than 14 °), it can be observed that the deformation of the membrane wing results in a smaller range of low-pressure areas on the upper surface of the wing and a greater lift towards the leading edge.

Figure 9 shows the Q-criterion vorticity contour of a rigid wing and a leading edge reinforced mixed membrane wing at different angles of attack, where a is the Q-criterion vorticity contour of the middle section position of the rigid wing, b is the Q-criterion vorticity contour of the middle section position of the leading edge reinforced mixed membrane wing, and c is the three-dimensional Q-criterion vorticity contour of the leading edge reinforced mixed membrane wing. Compared with the vorticity nephogram at the middle section of the rigid wing and the leading edge strengthened hybrid film wing under AOA=14 °, it can be seen that the vortex area on the upper surface of the rigid wing is large, and flow separation occurs on the upper surface, so the lift coefficient decreases; However, due to the deformation of the elastic membrane, the vortex area of the leading edge strengthened hybrid membrane wing is reduced, and the air flow is still attached to the upper surface of the wing. Therefore, the flow separation is not serious, and the lift coefficient remains large, delaying the occurrence of flow separation. Comparing the vorticity contour after stall, it can be seen that the vortex area of the leading edge reinforced mixed membrane wing is smaller than that of the rigid wing, and the deformation of the elastic membrane improves the aerodynamic performance after stall. According to the three-dimensional Q-criterion vorticity contour of the hybrid membrane wing with strengthened leading edge, flow separation first occurs at the wing root and gradually spreads to the wing tip as the angle of attack increases; The vortex region is concentrated at the position of the elastic film. For example, when AOA=14 °, except for the wing tip vortex, the vortex is mainly concentrated at the position of the elastic film near the wing root. When AOA=16 °, the vortex is mainly concentrated at the position of the elastic film near the wing root and in the middle, but the vortex near the wing root is larger. When AOA=18 °, the vortex is mainly concentrated at three positions of the elastic film, and gradually decreases from the wing root to the wing tip.

To evaluate the ability of the hybrid membrane wing with reinforced leading edge to resist spanwise bending and torsion deformation, it is also necessary to analyze the structural deformation displacement of the wing, as shown in Figure 10. It can be seen that as the angle of attack increases, the global deformation of the wing, as well as the displacement deformation of the leading edge and trailing edge of the wing tip, all increase. However, the displacement deformation of the leading edge of the wing tip is relatively small, with a maximum deformation of only 4.75%. This confirms that the leading edge reinforced hybrid membrane wing has good resistance to spanwise bending deformation. From the displacement contour, it can be seen that the deformation form of the wing is consistent, and the global maximum deforma-

http://www.imavs.org/

http://www.imavs.org/

tion comes from the deformation of the elastic membrane. The deformation of the elastic membrane is mainly caused by an upward protrusion in the middle, gradually increasing from the wing root to the wing tip. The small displacement deformation of the leading edge of the wing tip indicates that the hybrid membrane wing with strengthened leading edge has good resistance to spanwise bending deformation. The displacement deformation of the trailing edge of the wing tip is greater than that of the leading edge of the wing tip. The main reason is that the trailing edge of the wing tip is an arc-shaped flat wing and the Young's modulus of the elastic film is small, which reduces the stiffness of the trailing edge, but the deformation is small, indicating good resistance to torsional deformation.

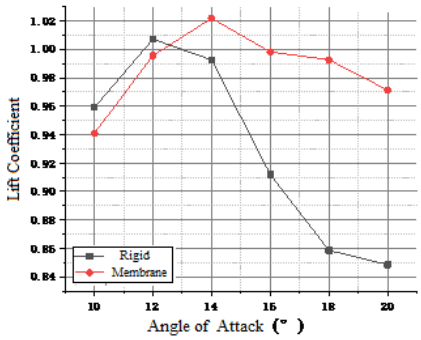

Figure 5: Lift coefficient varying with the angle of attack of the wing.

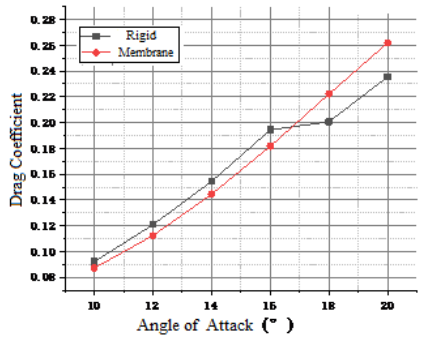

Figure 6: Drag coefficient varying with the angle of attack of the wing.

5 CONCLUSION

This paper proposes a leading edge reinforced membrane wing to address the issue of low spanwise stiffness and susceptibility to significant spanwise bending and torsion of membrane wings. The aerodynamic model and structural

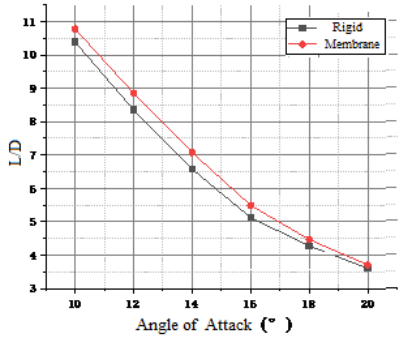

Figure 7: Ratio of the lift to drag varying with the angle of attack of the wing.

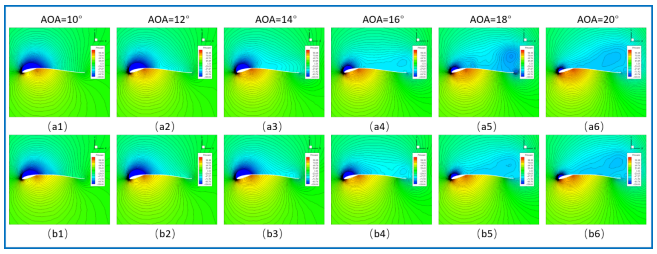

Figure 8: Pressure contour at the cross section of the wing.

model of the leading edge strengthened hybrid membrane wing were established. Based on the two-way fluid structure coupling model of the leading edge strengthened hybrid membrane wing, the aerodynamic and structural deformation analysis was carried out, and compared with the rigid wing, the results showed that the lift coefficient of the membrane wing before stall was less than that of the rigid wing, but the lift coefficient after stall was greater than that of the rigid wing, and the lift drag ratio of the membrane wing was greater than that of the rigid wing throughout the whole process, with higher aerodynamic efficiency. Analysis of struc-

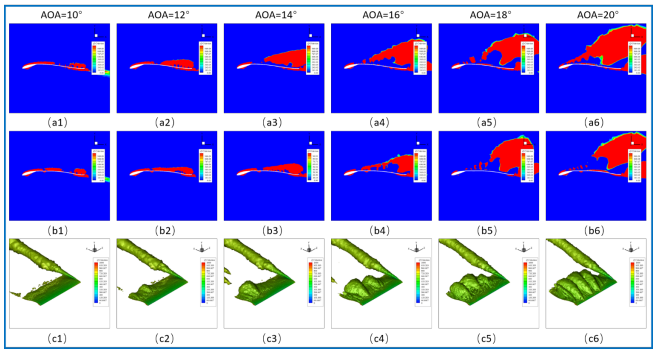

Figure 9: Q-criterion vorticity contour around the wing.

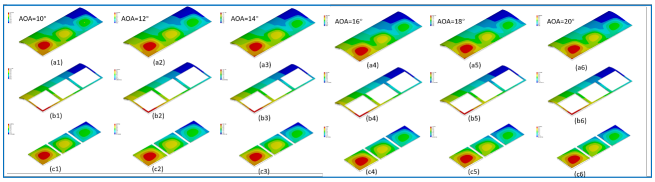

Figure 10: Structural deformation displacement contour of the wing.

tural displacement deformation found that the displacement deformation of the leading edge of the wing tip was relatively small, and the deformation of the wing mainly occurred in the elastic membrane part, verifying that the hybrid membrane wing with strengthened leading edge has good resistance to spanwise bending deformation. The results indicate that the leading edge reinforced hybrid membrane wing has good resistance to spanwise bending deformation, while retaining the adaptive passive deformation ability of traditional membrane wings, and has good stall performance.

In the further research work, it shall carry on wind tunnel tests to verify the simulation results.

ACKNOWLEDGEMENTS

The authors would like to thank the HPC center of the Xi'an Jiaotong University for their help on the simulation.

REFERENCES

[1] B. BEGUIN, C. BREITSAMTER, and N. ADAMS. Aerodynamic investigations of a morphing membrane wing. *AIAA Journal*, 50(11):2588–2599, 2012.

[2] M. D. Maughmer. *A Comparison of the Aerodynamic Characteristics of Eight Sailwing Airfoil Sections*. Princeton Univ, LLC, New York, NY, 1979.

[3] K. Fujita, K. Takahashi, and H.C. NAGAI. Permeable membrane wing characteristics at reynolds number order of 10,000. In *AIAA Scitech 2021 Forum*, 2021.

[4] R. M. WALDMAN and K. S. BREUER. Camber and aerodynamic performance of compliant membrane wing. *Journal of Fluids and Structures*, 68(1):390–402, 2017.

[5] A. SONG, X. TIAN, and E. ISRAELI. Aeromechanics of membrane wings with implications for animal flight. *AIAA Journal*, 46(8):2096–2106, 2008.

[6] A. Pelletier and T. J. Mueller. Low reynolds number aerodynamics of low-aspect ratio, thin/flat/cambered-plate wings. *Journal of Aircraft*, 37(5):825–832, 2008.

[7] G. E. Torres and T. J. Mueller. Low-aspect ration wing aerodynamics at low reynolds numbers. *AIAA Journal*, 45(5):865–873, 2004.

[8] R. ALBERTANI, B. STANFORD, and J. P. HUBNER. Aerodynamic coefficients and deformation measurements on flexible micro air vehicle wings. *Experimental Mechanics*, 47(5):625–635, 2007.

http://www.imavs.org/